Hexaferrite–FeCo nanocomposite particles and their electrical and magnetic properties at high frequencies

C. Sudakar, G. N. Subbanna,[a] and T. R. N. Kutty[b]
Materials Research Centre, Indian Institute of Science, Bangalore 560012, India

Nanocomposites are realized by chemical reduction whereby the conducting magnetic particles of Fe–Co alloy are generated within the insulating ferrimagnetic $BaCo_2Fe_{16}O_{27}$ or $Ba_2Co_2Fe_{12}O_{22}$ hexaferrite matrix. Transmission electron microscopy revealed that metal nanoparticles precipitate coherently as thin flakes along the $a-b$ planes of the derivative magnetoplumbite lattice of the hexaferrites above the characteristic reduction temperature, $T_R > 375\,^{\circ}C$ in H_2 atmosphere. The coercivity increases with T_R in the early stages of the solid-state precipitation and then decreases with the formation of larger fractions of Fe–Co alloy; a converse trend is noticed for magnetization. The complex permittivity increases with reduction to ~50 in the broad frequency range of 4–18 GHz. The complex permeability is also enhanced with the content of Fe–Co nanoparticles. It is proposed that the spin reorientation at the Fe–Co/hexaferrite interface gives rise to broadband response, rendering these composite particles useful as electromagnetic microwave absorbers.

I. INTRODUCTION

Composites, where the magnetic particles are usually embedded in either insulating or conducting matrix, are often employed in high speed electronic circuits to reduce the electromagnetic interference (EMI), decrease the noise level of signals and ensure the electromagnetic compatibility.[1] EM radiation shields, either reflection or absorption based, need be thin and lightweight, responsive to broader frequency range and nearly independent of the incident angle. As far as the thickness and working frequency bandwidth are concerned, the magnetic composites have definitive advantages over their dielectric analogues. The most commonly used fillers are spinel ferrites or hexaferrites. The latter with planar magnetic anisotropy are of great interest for use as electromagnetic energy dissipation materials in microwave frequency range.[2] $BaCo_2Fe_{16}O_{27}$ (WCo_2) and $Ba_2Co_2Fe_{12}O_{22}$ (YCo_2) hexaferrites are soft magnetic materials with planar anisotropy; they have relatively high resonance frequency and high permeability. However for broadband operation, magnetic nanocomposites are desirable. Nanosize iron particles dispersed in an oxide matrix by reaction milling have been studied.[3] However composite materials with conducting magnetic particles generated *in situ* by chemical reactions within the ferrimagnetic hexaferrite insulating matrix are scarcely known.

II. EXPERIMENT

In this article we report the structural, magnetic, and microwave absorption properties at very high frequencies (4–18 GHz) of the hexaferrite–FeCo alloy nanocomposites obtained by controlled chemical reduction of hexaferrite, WCo_2, and YCo_2. WCo_2 and YCo_2 hexaferrites with oriented grains were prepared by heat-treating at ~1250 °C the precursors obtained by the wet chemical gel-to-crystallite conversion.[4] Hexaferrite particles on controlled reduction in flowing hydrogen at 350–450 °C causes *in situ* precipitation of FeCo alloy (iron rich) nanoparticles within the hexaferrite matrix. Sample identifications used in the subsequent sections have been denoted with the type of hexaferrite followed by the heat-treatment condition in H_2. Thus, for example, WCo_2–R400 represents WCo_2 hexaferrite reduced at 400 °C. Phase identification of the powders was investigated by x-ray diffraction (XRD) using a Philips PW 1050 diffractometer equipped with Cu $K\alpha$ radiation. Metal content in the composite is evaluated by wet chemical analyses[5] as well by comparing the relative intensity of x-ray reflections of hexaferrite and iron from standard mixtures. Further, the compositional variations are evaluated by x-ray photoelectron spectra (XPS) of the samples with a VG ESCA 3 MK II instrument using Al $K\alpha$ x rays. Transmission electron microscopy observations were performed on the nanocomposites for morphological and lattice imaging studies, with a JEOL, JEM 200CX microscope. Magnetization measurements were carried out between −9 and +9 kOe at room temperature, by means of a vibrating sample magnetometer (VSM) (Lakeshore 7300). Complex permittivities ($\varepsilon' - j\varepsilon''$) and complex permeabilities ($\mu' - j\mu''$) were calculated from the measured reflection coefficients using the vector network analyzer (Agilent 8722 ES) in the frequency range of 4–18 GHz, wherein the samples are loaded in coaxial cells.

III. RESULTS AND DISCUSSION

Figure 1 shows the XRD patterns of WCo_2 and YCo_2 hexaferrites heat treated at 1250 °C. The relative intensities of WCo_2 x-ray reflections show oriented grain growth along certain crystallographic planes, predominantly (00l) reflec-

[a]Deceased on 16th July 2003.
[b]Author to whom correspondence should be addressed; electronic mail: kutty@mrc.iisc.ernet.in

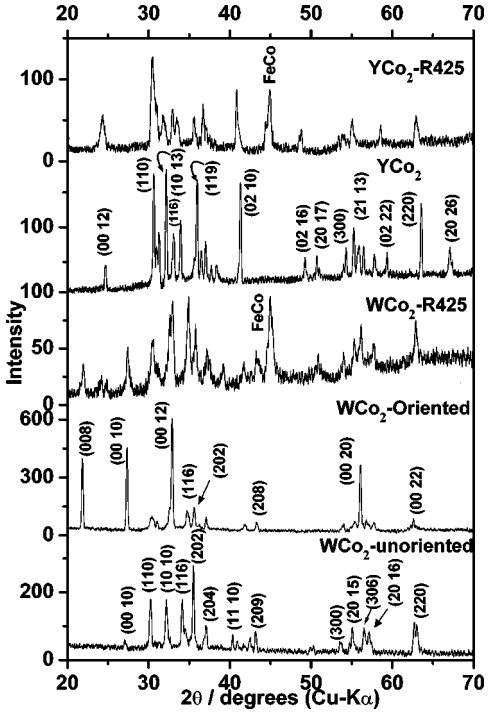

FIG. 1. XRD patterns of hexaferrites (WCo_2 and YCo_2) before and after reduction.

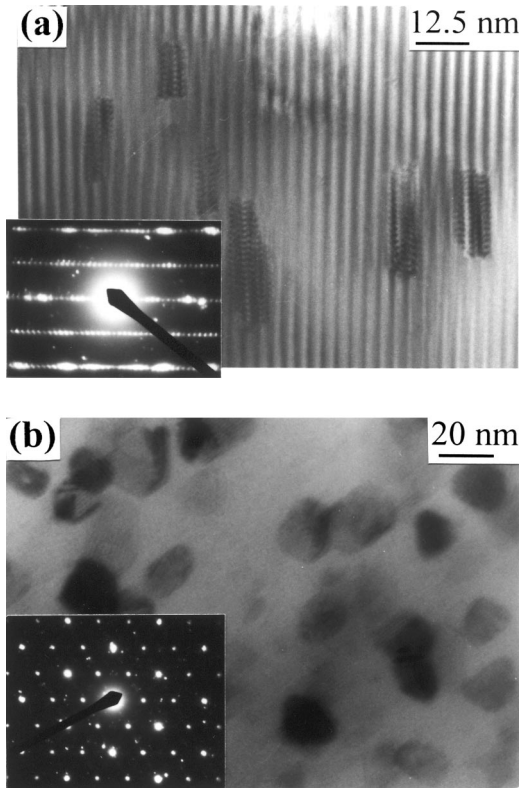

FIG. 2. High resolution electron micrographs of the WCo_2–R425 nanocomposite with beam direction along (a) [110] and (b) [001]. Corresponding SAED patterns are shown in the insets.

tions and (hkl) with larger l $(>h+k)$ as strong peaks, indicating that the particles are grown as platelets with the c axis nearly perpendicular to the plane of observation. The average grain size of the particles from scanning electron microscopy is $\sim$20 μm. The XRD patterns of YCo_2 also show narrow linewidths indicative of high crystallinity. On reducing these crystallites chemically at 350–450 °C in hydrogen atmosphere, reflections of Fe–Co alloy (bcc) show up in the XRD patterns along with those of hexaferrite. However, reflections of the latter become line broadened and the intensities decrease drastically with the extent of reduction. At $T_R \geqslant 450$ °C, the intensities of Fe–Co reflections increase. The characteristic temperature at which discernible reduction takes place, as observed from XRD and chemical analyses, differs for WCo_2 and YCo_2. WCo_2 has $\sim$5% FeCo formation at $T_R \cong 400$ °C (WCo_2–R400) for 1 h, whereas YCo_2 has the same percent of reduction at $T_R \sim 425$ °C (YCo_2–R425). Above these temperatures, the percentage of Fe–Co increases exponentially. The estimated (Fe–Co) content for samples heat treated at different temperatures in hydrogen atmosphere is given in Table I. The atomic ratio of Fe and Co estimated from XPS analyses in the reduced samples of WCo_2 is in the range of 6–8, whereas in YCo_2 it is around 4–6.

TABLE I. Estimated % of FeCo at different T_R and magnetic properties of WCo_2 and YCo_2 hexaferrites.

Sample Identification	T_R (°C)	% of FeCo (Fe/Co from XPS analyses)	M_S (emu/g)	H_C (Oe)
WCo_2–R375	375	-----	69.7	200
WCo_2–R400	400	4.9	62	247
WCo_2–R425	425	12.6 (7.5)	53	496
WCo_2–R450	450	17.8 (7.1)	50.5	581
WCo_2–R500	500	35 (6.5)	69	645
WCo_2–R700	700	75 (6.6)	169.7	52
YCo_2–R400	400	-----	35	205
YCo_2–R425	425	5.2	32.4	275
YCo_2–R450	450	14 (5.2)	30.8	437
YCo_2–R500	500	25 (4.6)	38.6	694
YCo_2–R700	700	54 (4.6)	122.6	72

Figure 2(a) shows the high resolution electron microscope image of the oriented hexaferrite particles (WCo_2) reduced at 425 °C. Uniform lattice fringes are discernible with regular coherent growth of the basic structural blocks in WCo_2, which are disturbed with the extent of chemical reduction. Just near the characteristic reaction temperature, $T_R \sim 400$ °C, the lattice images reveal embedded metal particles coherently growing along the $a-b$ planes. The metallic region expands with higher T_R ($\geqslant$425 °C). The lattice gets distorted as can be deciphered from the wrinkling of the lattice fringes due to stacking faults. This leads to further disintegration of the monocrystalline particles at $T_R \geqslant 450$ °C to composite multicrystallites of separate phases (Fe–Co alloy, BaO, and $BaFe_2O_4$). Interestingly, the reduced regions grow perpendicular to the c axis (along $a-b$ plane) of hexagonal magnetoplumbite structure. The high resolution image of a particle taken with the beam along the c axis reveals the internal structure of hexaferrite platelet with the embedded metal particle as thin nanoflakes [Fig. 2(b)]. The particles are well separated at $T_R \leqslant 425$ °C. The selected area

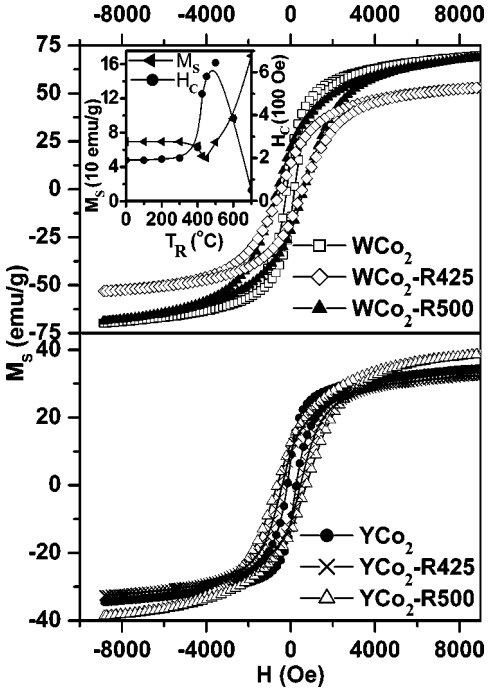

FIG. 3. M_S-H curves of WCo_2 and YCo_2 samples reduced at different T_R. Inset shows the variation of M_S and H_C with T_R for reduced WCo_2 hexaferrites.

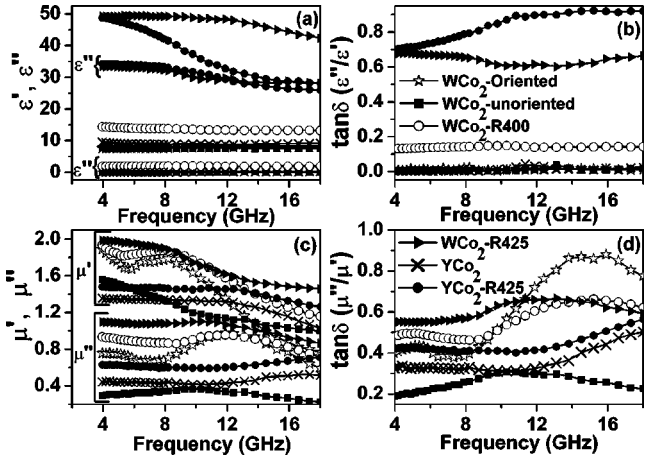

FIG. 4. Frequency dependence of (a) ε' and ε'', (b) tan $\delta(\varepsilon''/\varepsilon')$, (c) μ' and μ'', and (d) tan $\delta(\mu''/\mu')$ of WCo_2 and YCo_2 before and after reduction.

electron diffraction (SAED) of such composites show very feeble reflections from the embedded metal nanoparticles. Similar observations were made with Y–Co_2 hexaferrite as well. However, the metal particles grow and coalesce, followed by the disintegration of the matrix at higher T_R.

The particles with composite characteristics, namely the hexaferrite matrix still remaining intact with minimum defects and the coherent flaky metallic phase (FeCo alloy) precipitated *in situ*, give rise to modified magnetic properties as well as microwave absorption in contrast to the corresponding bulk phases. The variation of magnetization as a function of applied magnetic field for differently reduced samples is shown in Fig. 3. For W–Co_2 hexaferrite, the as-prepared particles have specific magnetization, $M_S = 69.7$ emu/g and coercivity, $H_C = 190$ Oe, whereas samples reduced at 400 °C in H_2 have $M_S \approx 62$ emu/g and $H_C \approx 250$ Oe. For WCo_2–R425 M_S decreases further to ~53 emu/g, whereas H_C increases to ~500 Oe. The decrease in M_S can be understood from the formation of defective hexaferrite matrix with nanocrystalline Fe–Co particles. On the other hand, the coercivity of the particles increased due to the pinning of the domains by the presence of defects. Thus, the composites exhibit combination dependent magnetic property rather than contributions from the individual components. For samples reduced at 500 °C, M_S increases to 69 emu/g with H_C further increasing to 645 Oe. The increase in M_S results from the larger amounts of coarser Fe–Co alloy formation. The increasing trend of coercivity indicates that the defects still play a role in pinning down the domain reversals in the ferrimagnetic components. The trend of changes in M_S and H_C with the T_R is shown clearly in the inset of Fig. 3. For deeply reduced samples (at ~700 °C) the magnetization increases enormously (~169 emu/g), indicating ~75% (by weight) constitute the metallic FeCo particle. Y–Co_2 hexaferrites reduced in H_2 display nearly similar changes (Fig. 3). The magnetic properties of reduced samples of YCo_2 hexaferrites are listed in Table I. The as-prepared samples of Y–Co_2 have $M_S = 35$ emu/g and $H_C = 205$ Oe. The coercivity initially increases with the T_R (<500 °C) and then decreases with the precipitation of more Fe–Co in the composite. Magnetization decreases when $T_R \leqslant 450$ °C, with a reversing trend when the samples are reduced at higher temperatures.

The complex dielectric as well as magnetic properties of the ferrite powders are measured in the region of 4–18 GHz. The dielectric properties of the samples do not show significant changes in comparison to the bulk at these frequency ranges [Figs. 4(a) and 4(b)]. However, the properties differ for the hexaferrites after reduction. The as-prepared powders have real part of complex permittivity (ε') around 7–8 and the imaginary parts (ε'') of 0.1–0.3 for WCo_2 and YCo_2. The ε' increases with the extent of reduction. For WCo_2–R400, ε' increases to ~12 and further to ~50 for WCo_2–R425. ε' decreases with increasing frequency for WCo_2–R425 and YCo_2–R425. The imaginary part of permittivity (ε'') also shows an increase to ~30 for these samples. For the as-prepared samples, the dielectric loss tangent (tan $\delta = \varepsilon''/\varepsilon'$) is very small with near zero values, whereas, tan δ is high for reduced samples. The real (μ') and imaginary (μ'') parts of relative complex permeability are shown in Figs. 4(c) and 4(d), wherein μ' decreases with frequency in all samples owing to the broadening of ferrimagnetic resonance. The magnetic resonance behavior is better discernible in oriented WCo_2 and YCo_2 grains. The natural resonance frequency due to spin rotation is around 12–13 GHz for WCo_2 and ~18 GHz for YCo_2, corresponding to the maximum observed in μ'' frequency curves. These samples have larger values of magnetic loss tangent (tan $\delta = \mu''/\mu'$) in the vicinity of the resonance frequency, whereas for unoriented crystals, μ'' is low (~0.3) with shallow magnetic loss and the resonance is discernible around 8–10 GHz. The magnetic loss spectra have similar changes with μ'' and have the highest absorption loss just above the resonance frequency, where the loss tangent is maximum. The maxi-

mum magnetic loss is observed for oriented W–Co_2 hexaferrite at ~15 GHz. For reduced samples, permeability increases slightly with the reduction temperature. The larger permeability in the high frequency region for the composite particles in which the flaky thin metal nanoparticles are oriented in the $a-b$ planes of the hexagonal platelets, results from the anisotropic morphology of the constituent particles. Thus, the hexaferrite metal nanoparticle composites show considerably smaller reluctance in the oriented directions than the unoriented particle system. The high permeability of the magnetic composite over a broad range of frequency (4–18 GHz) makes it possible to produce thinner electromagnetic wave absorbers. The magnetic structure at the metal/hexaferrite interface in the composite, with magnetization direction dictated by the combined anisotropy fields of the ferrimagnetic components, can lead to its own characteristic relaxation processes due to complex spin reorientation at high frequencies. Thus the magnetic loss spectra show broad absorption from 4 to 18 GHz.

IV. CONCLUSION

In conclusion, composites of hexaferrites containing Fe–Co alloy (iron rich) nanoparticles precipitated *in situ* are good candidates for wide bandwidth electromagnetic microwave absorption in broad frequency ranges. Such nanocomposites are easier to prepare when compared to iron particle dispersed in oxide matrix by mechanochemical milling.

ACKNOWLEDGMENT

The Board for Smart Materials Research and Technology of NPSM, Government of India, is thanked for the research funding.

[1] S.-H. Yu and M. Yoshimura, Adv. Funct. Mater. **12**, 9 (2002).
[2] T. Inui, K. Konishi, and K. Oda, IEEE Trans. Magn. **35**, 3148 (1999).
[3] M. Pardavi-Horvath, J. Magn. Magn. Mater. **215–216**, 171 (2000).
[4] C. Sudakar, G. N. Subbanna, and T. R. N. Kutty, J. Magn. Magn. Mater. **263**, 253 (2003).
[5] A. I. Vogel, *Textbook of Quantitative Chemical Analysis*, 5th ed. (Longman, Singapore, 1991), p. 376.